Biomass pyrolysis experiments in an analytical entrained flow reactor between 1073 K and 1273 K

Capucine Dupont, Jean-Michel Commandre, Paola Gauthier, Guillaume Boissonnet, Sylvain Salvador, Daniel Schweich

Biomass pyrolysis experiments in an analytical entrained flow reactor between 1073 K and 1273 K

Capucine Dupont [a,*], Jean-Michel Commandré [b], Paola Gauthier [a], Guillaume Boissonnet [a], Sylvain Salvador [b], Daniel Schweich [c]

[a] CEA Grenoble, DTN/SE2T/LPTM, 17 rue des Martyrs, 38054 Grenoble Cedex 09, France
[b] RAPSODEE, Ecole des Mines d'Albi-Carmaux, Campus Jarlard, 81013 Albi Cedex 09, France
[c] LGPC, CNRS-ESCPE, 43 bd du 11 Novembre, BP 2077, 69616 Villeurbanne Cedex, France

Abstract

Experiments are performed in an entrained flow reactor to better understand the kinetic processes involved in biomass pyrolysis under high temperatures (1073–1273 K) and fast heating condition (>500 K s^{-1}). The influence of the particle size (0.4 and 1.1 mm), of the temperature (1073–1273 K), of the presence of steam in the gas atmosphere (0 and 20 vol%) and of the residence time (between 0.7 and 3.5 s for gas) on conversion and selectivity is studied. Under these conditions, the particle size is the most crucial parameter that influences decomposition. For 1.1 mm particles, pyrolysis requires more than 0.5 s and heat transfer processes are limiting. For 0.4 mm particles, pyrolysis seems to be finished before 0.5 s. More than 70 wt% of gas is produced. Forty percent of the initial carbon is found in CO; less than 5% is found in CO_2. The hydrogen content is almost equally distributed among H_2, H_2O and light hydrocarbons (CH_4, C_2H_2, C_2H_4). Under these conditions, the evolution of the produced gas mixture is not very significant during the first few seconds, even if there seems to be some reactions between H_2, the C_2 and tars.

Keywords: Biomass; Flash pyrolysis; Gas yields

1. Introduction

The physical and chemical mechanisms involved in biomass steam gasification are still poorly understood, especially under high temperatures (1073 K < T < 1273 K) and high heating rate (>500 K s^{-1}). The present work consists of analytical experiments that should help to better understand the processes occurring at the particle scale during the first seconds of the transformation. This first stage is called "pyrolysis" in our study and gathers both biomass decomposition, often called "primary pyrolysis", and the secondary reactions of the vapours produced during primary pyrolysis. The experiments are performed in a free-fall reactor, also called entrained flow reactor (EFR). This reactor is an interesting analytical tool to study the global reaction of flash pyrolysis [1–13], since very high heating rates of the particles can be obtained. Moreover, the residence time can be varied over a range of a few seconds, and the particles can be assumed to be isolated from each other, which makes interpretation easier [1,14]. Up to now, few experiments have been performed under the operating conditions of interest, the most complete set of data being given by Zanzi [5].

Section 2 is devoted to the description of the experiments. Results are shown and discussed in Section 3. Eventually, conclusions are drawn in Section 4.

* Corresponding author. Tel.: + 33 4 38 78 02 05; fax: + 33 4 38 78 52 51.
E-mail address: capucine_dupont@hotmail.fr (C. Dupont).

2. Description of the experiments

2.1. Biomass samples

The biomass used in this study is a mixture of two softwoods (sylvester pine and spruce). Two particle sizes are considered: 355–530 μm, called 0.4 mm and 1.00–1.25 mm, called 1.1 mm. The data on biomass samples are given in Table 1.

2.2. Experimental facility

The entrained flow reactor is shown in Fig. 1. A complete description of the apparatus and its thermal and hydrodynamic characterization were given in previous works from Van de Steene [4] and Commandré [14].

The reactor is made up of an alumina tube heated by an electric furnace that can reach 1273 K. Feed gas was either pure N_2 or a mixture of 80% N_2 and 20% steam. The gas is injected at the top of the reactor with a flow rate of 16 L min^{-1} (STP) and then passes through an electric preheater. The solid particles are injected at the top of the reactor by pneumatic transport (flow rate of $N_2 = 2$ L min^{-1} (STP)) in a tube which is cooled by thermal oil. The solid flow rate is 1 g min^{-1}, which ensures that particles may be assumed to be isolated from each other. A dispersion dome is placed at the outlet of the cooled tube, in order to distribute the particles as homogeneously as possible over the reactor cross-section. Under the explored conditions, flow is laminar ($Re < 2000$). Measurements have shown that the reactor is isothermal in the zone between 0.30 and 0.95 m away from the solid injection.

A sampling probe cooled by thermal oil is placed from bottom at different heights inside the reactor and aspirates a representative part of the gases and solids for analyses. Thus the residence time inside the reaction zone is controlled. Its calculation for solid takes into account the

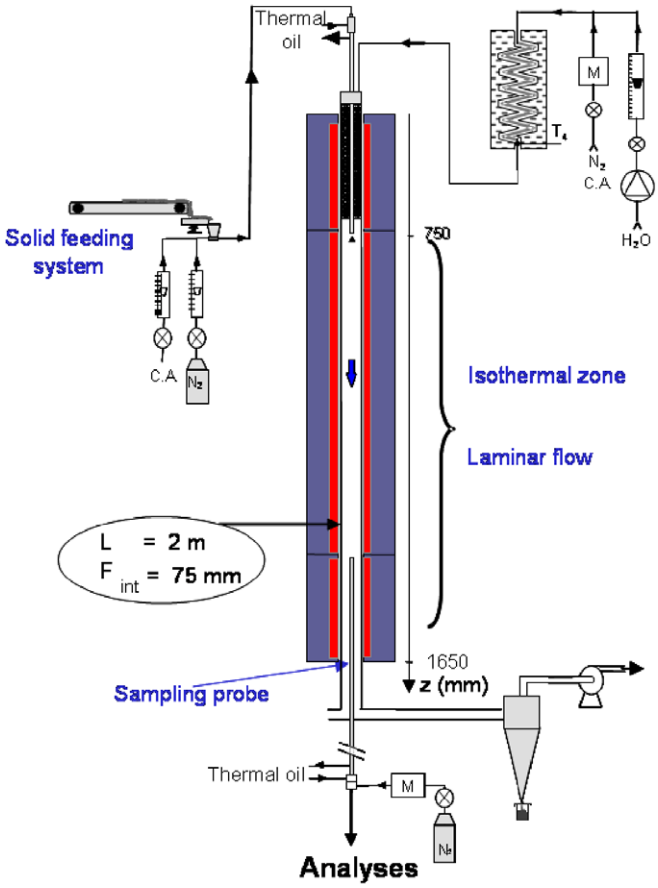

Fig. 1. The entrained flow reactor (EFR).

Table 1
Data on biomass samples

		Units	Measurement method	Sample 0.4 mm	Sample 1.1 mm
Ultimate analysis	Carbon	wdaf %[a]	NF M03–032	48.6	50.5
	Hydrogen	wdaf %	NF M03–032	6.0	6.25
	Nitrogen	wdaf %	NF M03–018	0.2	0.1
	Sulfur	wdaf %	NF EN 14 582	0.03	0.02
	Oxygen	wdaf %	By difference	43.0	43.1
	Elemental formula			$C_6H_{8.8}O_{3.9}$	$C_6H_{8.8}O_{4.0}$
Proximate analysis	Moisture	w%	NF M03–002	7.2	8.6
	Volatile matter	wdf %[b]	NF M03–004	77.0	77.4
	Fixed carbon	wdf %	NF M03 006	20.9	21.9
	Ash	wdf %	NF M03–003	2.1	0.6
Main components	Cellulose	wdaf %	[c]	44.5	Not measured
	Hemicelluloses	wdaf %	[c]	21.0	Not measured
	Lignin	wdaf %	[c]	24.9	Not measured
	Extractives	wdaf %	[c]	9.6	Not measured
	Skeletal density	–	Helium picnometer	1.46	Not measured
	Particle density	–		0.3	

[a] wdaf %: mass percent dry ash free.
[b] wdf %: mass percent dry free.
[c] There is no universal standard for main components measurements. The results for cellulose, hemicelluloses and lignin are the mean values of measurements made in three different laboratories with different methods. The total is brought to 100%.

Table 2
List of experiments

Particle size (mm)	Steam in feed gas (vol%)	Temperature (K)	Solid residence time (s)
0.4	0	1073; 1173; 1273	0.35; 0.45; 0.55; 0.75; 1.00
	0; 20	1073; 1223	
1.1	0	1073; 1223	0.30; 0.40; 0.45

particle slip velocity, which is comparable with the gas velocity for 0.4 mm particles and about ten times higher than gas velocity for 1.1 mm particles.

The sampled part is sent to a pot in which the solid residue is collected, then the gas mixture is sent to a filter that retains fine particles and most remaining tars. The sampling line is heated up to a condenser which is cooled ($T = 275$ K) by a glycol–water mixture. This condenser is used to collect most of the water contained in the gas. At the outlet of the condenser, the gas is analyzed by a Fourier transformed infra red (FTIR) spectrometer (CO, CO_2, CH_4, C_2H_4, C_2H_2, C_2H_6), a paramagnetic analyser (O_2), two Flame Ionisation Detectors (FID) (CH_4, total hydrocarbons), a TCD (H_2) and an hygrometric mirror (H_2O contained in gas at ambient temperature). Hydrocarbons between C_3 and C_6 and tars are not measured. The mass of solid residue is calculated through the ash tracer method, whose principle is explained in detail in [15].

The main operating conditions of the experiments are summarized in Table 2.

2.3. Mass and elemental balances

Mass balances are made over the collected gas and the solid recovered in the collecting pot. The balances are satisfied within about 10 wt% uncertainty for each experiment. As far as elements (C, H, O) are concerned, about 20% of the initial carbon and 20% of the initial hydrogen are missing, whereas only 5% of the initial oxygen is missing. The formula of the missing mass is therefore $C_6H_6O_{1.5}$. This formula is quite similar to the mean formula (C_6H_4O) of the products collected in the sampling line filter and to the formula of the main component of the tars collected under the condenser (phenol C_6H_6O). Consequently, it may be assumed that this missing mass could be partly attributed to light hydrocarbons (C_3 to C_6) and tars that are not measured in these experiments.

In similar experiments found in the literature, the tar content in products is found to be from 4 wt%, including C_6H_6 [5], to 15 wt% [11]. Thus it seems quite reasonable to assume a tar yield of 10 wt% in our experiments. Note that this relatively important difference between tar contents after similar experiments may be explained by the difference in solid residence time among the experiments. This may influence the extent of tar cracking and consequently the tar content in products.

3. Results and discussion

Within the range of study, the most influential parameter on the results is the particle size. That is the reason why the results are separated into two sub-sections, each one being devoted to one particle size.

3.1. 0.4 mm particles

3.1.1. Results on the solid residue

3.1.1.1. Observations on the residue. Fig. 2 shows ESEM pictures of the initial biomass and of solid residue obtained at 1073 K under N_2 atmosphere and a solid residence time of 1.0 s. The solid residue is made up of two different kinds of particles shown in Fig. 3:

- Particles that have kept the fibrous structure of wood and the aspect of thick slabs;
- Particles that have completely lost the initial wood structure and that look like exploded spherical shells of reduced size (about 0.1 mm), with small pores on their walls.

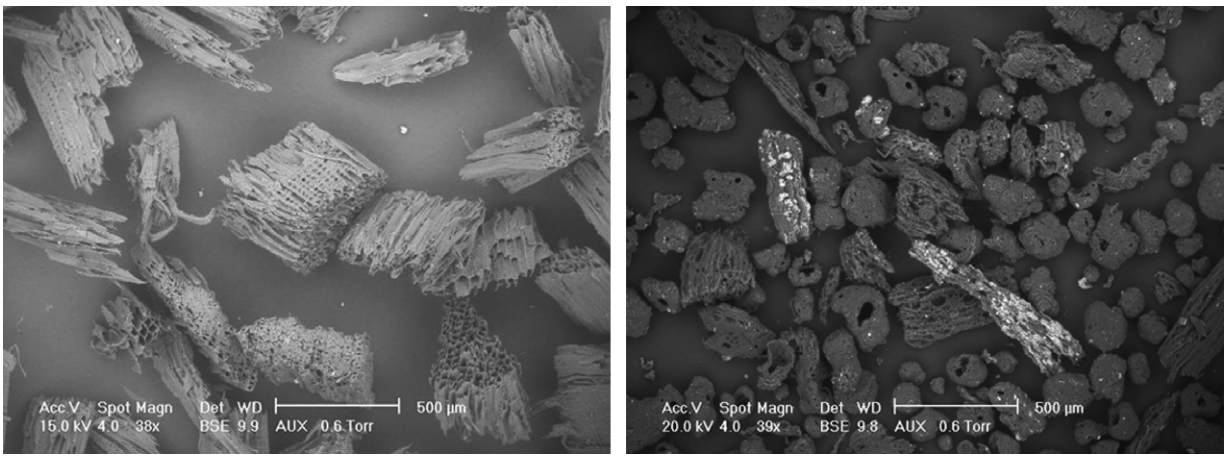

Fig. 2. Left: initial wood (0.4 mm); Right: residue obtained after an experiment (100% N_2; 1073 K; solid residence time: 1.0 s).

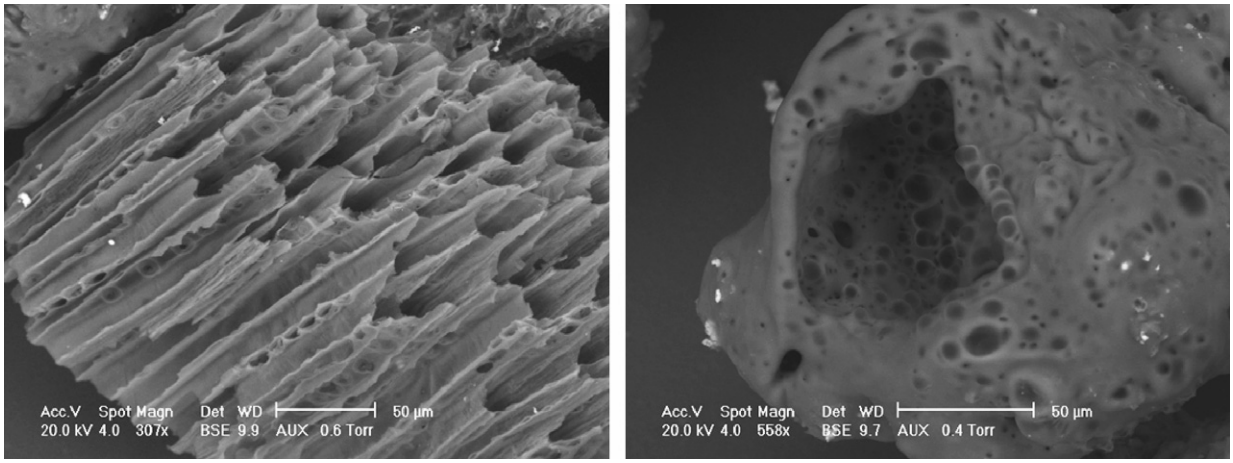

Fig. 3. Left: fibrous residue; Right: porous residue (100% N_2; 1073 K; solid residence time: 1.0 s).

Only the second type of particles is mentioned in the literature on flash pyrolysis at high temperatures [5,16]. The destruction of the initial fibrous structure is generally explained by an important pressure increase inside the particle due to the fast expulsion of a large amount of volatile compounds. From the analysis of the surface composition, it was stated that the outer surface of the two kinds of particles is mainly made of carbon, with very low oxygen content. This proves that even the fibrous particles are not wood anymore but solid residue.

Note that small white spots can be seen in residues in Fig. 2. They are constituted of inorganic components, mainly Si, Ca and also K, Na or Fe for example. These components are under their oxidised form since much oxygen is measured. Their origin may be the inorganic components initially contained in biomass, and lumped into the term "ash". During the transformation, they may undergo fusion phenomena. This would be coherent with the observations on wood done by some authors at temperatures from 1073 K to 1273 K [17,18]. Moreover, as can be seen in Fig. 4, there are much more mineral parts on the surfaces

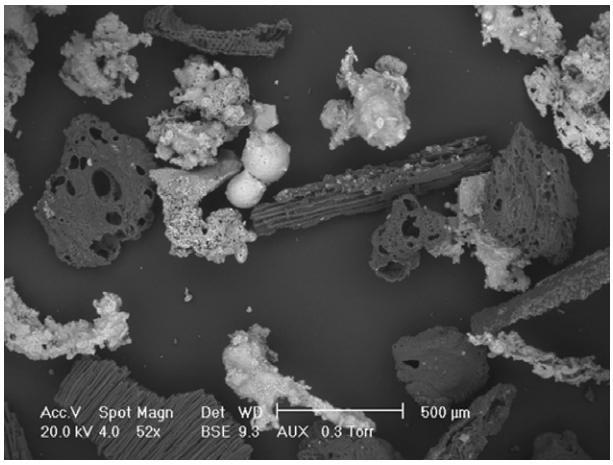

Fig. 4. Residue obtained at 1273 K (100% N_2; solid residence time: 1.0 s).

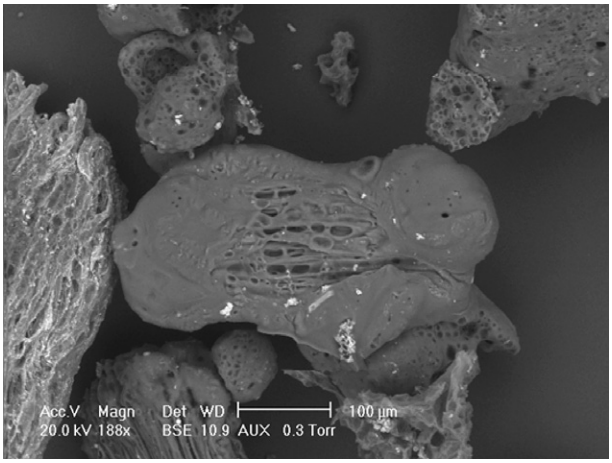

Fig. 5. Residue obtained after 0.5 s (100% N_2; 1073 K).

of the particles that were pyrolysed at the highest temperature, i.e., 1273 K. This is in agreement with the observations of Zanzi [5]. This higher proportion of inorganic matter in residue may be due to the higher consumption of organic matter during the reaction.

At short residence times, of about 0.5 s, as shown in Fig. 5, some particles seem to be heterogeneous. They keep a fibrous structure on some parts, whereas they show a molten coating frozen into a porous shell on other parts. The boundary between the two parts of the particles looks like a frozen liquid, as if a fusion phenomenon had occurred. This observation seems logical in so far as biomass is a polymer. Moreover, this would be in agreement with the "fusion-like phenomenon" of wood stated by Lédé [19] and the existence of an intermediate liquid compound (ILC) proven in case of cellulose by Boutin [20].

3.1.1.2. Elemental composition of the residue. The ratio of Hydrogen to Carbon in the solid residue H/C is plotted versus solid residence time for different temperatures in

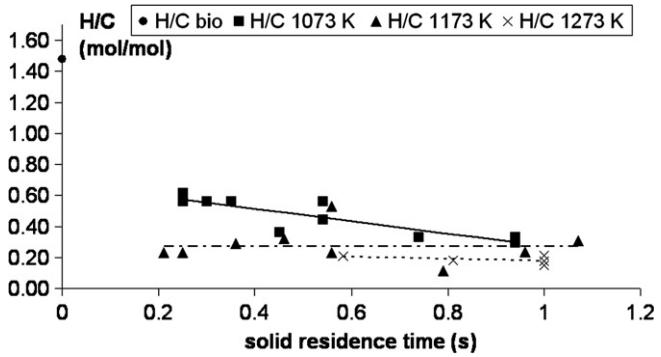

Fig. 6. H/C ratio of solid residue versus solid residence time in the temperature range 1073–1273 K.

Table 3
Mean gas yields and standard deviations for pyrolysis experiments on 0.4 mm particles

	Mean gas yield (standard deviation)	
	mol% of wet gas	w% of dry biomass
H_2	20.9 (6.5)	1.8 (0.7)
CO	44.4 (3.8)	53.4 (2.4)
CO_2	3.0 (0.5)	5.7 (1.0)
CH_4	7.9 (1.5)	5.4 (0.8)
C_2H_4	2.3 (1.2)	2.7 (1.3)
C_2H_2	2.5 (0.6)	2.8 (0.9)
C_2H_6	0.0 (0.0)	0.0 (0.0)
H_2O	19.0 (4.7)	14.6 (3.8)

Fig. 6. The value for the initial biomass is given as the black dot on the vertical axis.

The trend shows that the pyrolysis process is finished for a residence time greater than about 0.3 s provided the temperature is greater than or equal to 1173 K. In this case, the chemical formula of the residue is $C_6H_{1.5}O_{0.4}$. For 1073 K, the decreasing trend suggests some kinetically limiting process. At this temperature, the chemical formula of the residue is $C_6H_{2.7}O_{0.8}$ for the longest residence time.

3.1.2. Gas–solid distribution

As can be seen in Fig. 7, more than 75 wt% of the initial biomass is converted into wet gas and the amount of solid residue is low, of about 7–10 wt%, whatever the operating conditions are (1073 K $< T <$ 1273 K; solid residence time between 0.3 and 1.0 s). This is in agreement with Zanzi's results on wood (78 wt% at 1073 K and 87 wt% at 1273 K), and confirms that the decomposition of 0.4 mm particles is near completion after 0.3 s for temperatures greater than 1073 K.

Since the amount of residue after pyrolysis is very low, if it were fully available for the reaction of gasification with steam, this would increase the global conversion of biomass into gas of 10 wt% only, which remains relatively low. Thus, under the conditions of study considered here, the gas composition is mainly determined by the biomass pyrolysis process and the possible gas phase reactions, and not by the steam gasification of the solid residue.

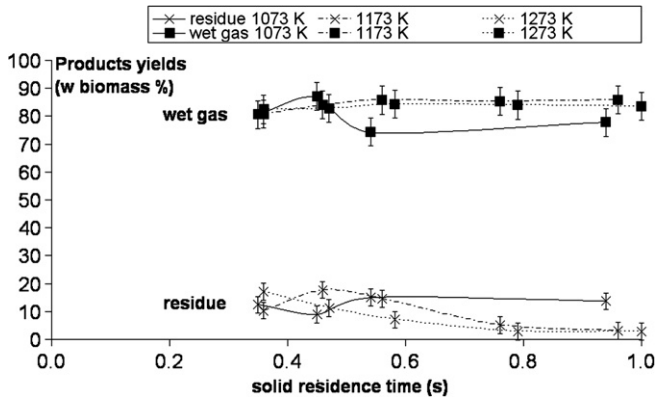

Fig. 7. Yields of wet gas and residue versus solid residence time in the temperature range 1073 K–1273 K.

3.1.3. Mean gas yields

The standard deviations on the gas yields have been calculated from the whole set of experiments performed under pure N_2. As can be seen in Table 3, they are quite small on most major gases, namely CO, CO_2 and CH_4. They are a little higher on H_2, C_2 species and H_2O. Globally speaking, it can be concluded that the gas composition is not very sensitive to the tested parameters (1073 $< T <$ 1273 K; residence time: 0.3–1.0 s).

In this context, it is interesting to have a look at Fig. 8 which gives the distribution in the products of the elements C, H and O initially contained in biomass for a typical experiment ($T = 1173$ K; solid residence time = 1.0 s; 100% N_2). It can be seen that about 50% of the initial carbon is converted into CO. Less than 5% is found in CO_2, leading to a molar ratio CO_2 to CO below 0.1. The trend is the same in Zanzi's tests, but not so strongly marked, with a ratio of about 0.2. It is interesting to note that the result is different in steam gasification experiments performed in fluidised bed. In this case, as shown in [21], the ratio is about 1. This may be explained by the difference in the solid residence time between the two types of reactors. Thus, the extent of the gas phase reactions, notably the water–gas shift, may be different.

H_2 and H_2O are the other main gases, each one containing about 25% of the hydrogen initially contained in biomass. As explained above, about 20% of hydrogen is not recovered and this may be partly attributed to light hydrocarbons between C_3 and C_6 and tars. The remaining 30% are converted into CH_4, C_2H_2 and C_2H_4. Among these three species, CH_4 is the major one, while C_2 species amount up to 10% of the initial carbon and hydrogen.

3.1.4. Gas yields versus temperature and residence time

Gas yields are plotted for different temperatures versus solid residence time in the range [1073–1273 K] in Figs 9–11.

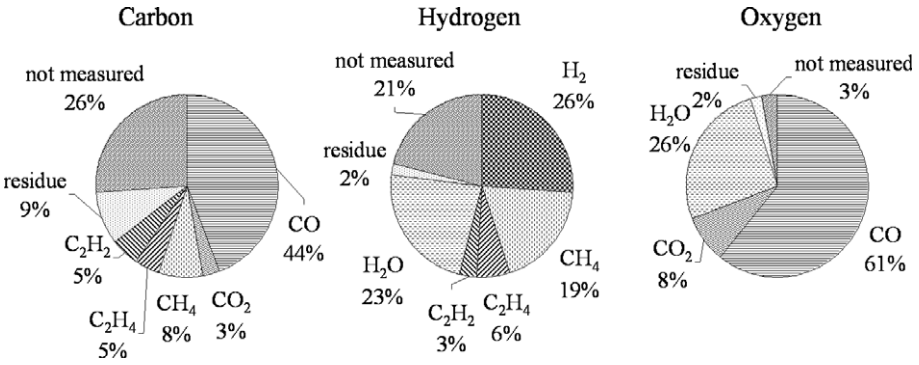

Fig. 8. Distribution of the elements C, H, O in the products for a typical pyrolysis experiment on 0.4 mm particles ($T = 1173$ K; solid residence time = 1.0 s; 100% N_2).

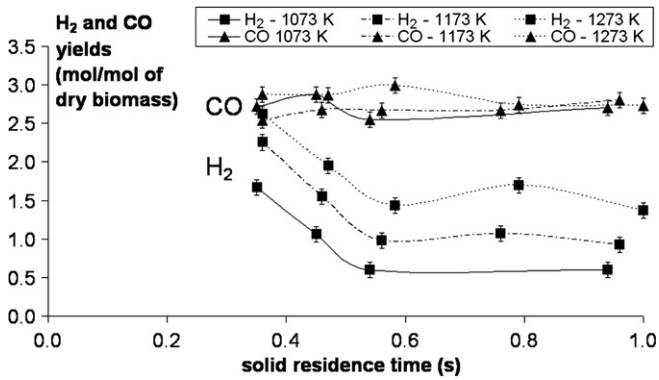

Fig. 9. H_2 and CO yields versus solid residence time in the temperature range 1073 K–1273 K.

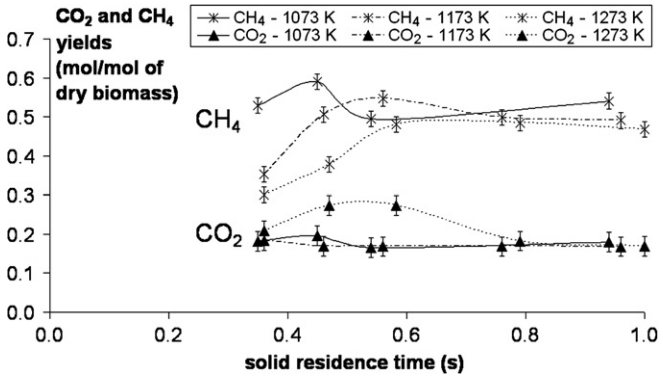

Fig. 10. CO_2 and CH_4 yields versus solid residence time in the temperature range 1073 K–1273 K.

To explain the trends observed on the graphs, two assumptions are made. Firstly, the solid decomposition is finished before 0.35 s, which seems justified if we refer to the results on the solid residue shown in the previous sections. Secondly, the gas–solid reactions are too slow to occur inside the reactor under the conditions of the study. Therefore, the evolutions of the gas phase composition may only be attributed to homogeneous reactions (including the reactions involving tars).

In [15], it has been proposed to describe the gas phase by the five main species (H_2, CO, CO_2, CH_4, H_2O) and two independent reactions:

- The steam reforming of CH_4, which seems to be kinetically blocked under these conditions ($1073\ \text{K} < T < 1273$ K; residence time of a few seconds).
- The water–gas shift, which seems to need more than 10 s to attain equilibrium at 1073 K, and which is at equilibrium at 1273 K.

For these two reactions, the equilibrium constant can be compared with the reaction constant calculated with the partial pressures of the different gases from the experiments. This should enable to check the validity of the theoretical assumptions. Results obtained at different temperatures are shown in Table 4.

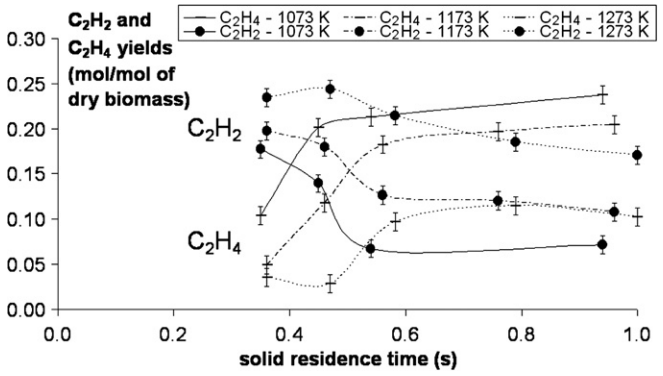

Fig. 11. C_2H_2 and C_2H_4 yields versus solid residence time in the temperature range 1073 K–1273 K.

As expected, the steam reforming of CH_4 is far from equilibrium within this range of temperatures. The water–gas shift does not reach equilibrium under the conditions of the experiments, even if the ratio between the reaction constant and the equilibrium constant is closer to 1 at 1273 K. These results are in agreement with those of Zanzi [5], obtained in a free-fall reactor under comparable conditions to ours. On the contrary, at the same temperatures, the water–gas shift seems to be at equilibrium in fluidised

Table 4
Comparison between experimental reaction constant and equilibrium constant of water–gas shift and steam reforming of CH_4

Temperature	K	1073	1273
Gas residence time	s	3.2	3.2
Water–gas shift			
$K_{\text{shift exp}}$	–	0.05	0.19
$K_{\text{shift éq}}$	–	1.04	0.57
$K_{\text{shift exp}}/K_{\text{shift éq}}$	–	0.05	0.32
Steam reforming of CH_4			
$K_{\text{ref}CH_4\text{eq}}$	–	0.06	0.7
$K_{\text{ref}CH_4\text{exp}}$	–	170	9280
$K_{\text{ref}CH_4\text{exp}}/K_{\text{ref}CH_4\text{eq}}$	–	3.4×10^{-4}	7.3×10^{-5}

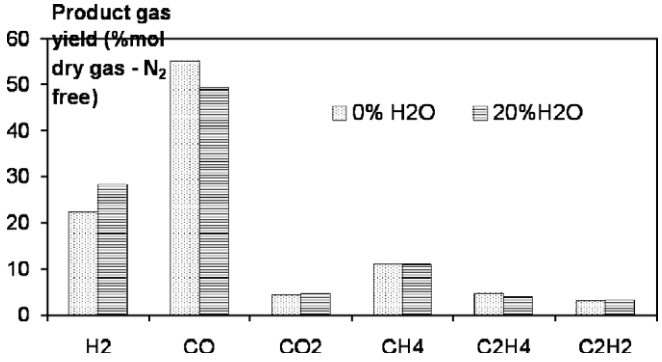

Fig. 12. Product gas yield versus presence of steam in the feed gas ($T = 1223$ K; solid residence time = 0.5 s).

bed if we refer to literature results [22] and to experimental results obtained recently at 1073 K in a fluidised bed built in our laboratory [23]. The gas residence time is of about 10–100 s in fluidised bed, which would mean that the water–gas shift has a characteristic time of about 10–100 s within the range of temperatures 1073–1273 K. Thus, this implies that the water–gas shift has to be considered as kinetically limited within the range of temperatures 1073–1273 K when the gas residence time is shorter than 10 s.

The H_2 yield is clearly favoured from 1073 K up to 1273 K, with a total increase of about 1 mol/mol of dry biomass. Between 0.3 and 0.55 s, there is a strong decrease of the amount of H_2, of about 1 mol/mol of dry biomass, that is, more than 50% of the total yield of H_2. If only the five main species are considered, the evolutions observed on H_2 with temperature and residence time cannot be explained.

If we compare H_2 and C_2 species, they clearly seem to be correlated. H_2 and C_2H_2 follow similar trends, whereas C_2H_4 evolves symmetrically to them. Based on these observations, the assumption can be made that the following reaction of hydrogenation occurs inside the reactor:

$$C_2H_2 + H_2 \rightleftharpoons C_2H_4 \quad (1)$$

Since the reverse reaction is thermodynamically favoured when temperature increases, this could explain why C_2H_4 tends to decrease with temperature in favour of C_2H_2. However, quantitatively speaking, this reaction can only explain about 10% of the decrease observed on H_2 with residence time. It may be suggested that other reactions also occur involving H_2 and heavier hydrocarbons.

Finally, it seems that the only homogeneous reactions that have enough time to occur inside the reactor under these conditions of temperature would be the reactions between the hydrocarbons and H_2.

3.1.5. Gas yields in the presence of steam

Dry gas yields are given in Fig. 12 for experiments performed under pure N_2 and a mixture of 80 vol% N_2 + 20 vol% H_2O at 1223 K for a solid residence time of 0.5 s. The trends are similar at 1073 K and other residence times in the range tested [0.3;1.0 s].

The presence of steam clearly influences the yields of H_2 and CO. The amounts of the other gases do not seem to be significantly affected. Quantitatively, the increase of H_2 yield, of about 6 mol%, seems to be well-balanced by the decrease of CO. This can be explained by the water–gas shift reaction. However, this would imply a correlative increase in CO_2 yield, which is not observed. To explain this discrepancy we need to invoke a heterogeneous reaction with the residue, namely:

$$C + CO_2 \rightleftharpoons 2CO \quad (2)$$

It is well-known that under the studied conditions of temperature, this reaction is strongly kinetically limited [24]. We have thus no satisfactory explanation for the contradictory behaviours of H_2, CO and CO_2. Even artefacts such as CO_2 dissolution in the water condensed during the experiments is not convincing.

The absence of the influence of steam on CH_4 confirms that the steam reforming of CH_4 is kinetically blocked under our conditions. The same assessment can be made about the steam reforming of C_2H_2 and of C_2H_4, since their yields are not modified by the presence of steam. The steam cracking of heavier hydrocarbons may occur, since these products are less stable than CH_4 or C_2 species. This could explain the increase of H_2 yield, but these reactions would also produce CO, which is contradictory with its decrease.

3.2. 1.1 mm particles

3.2.1. Preliminary remark

The experiments on 1.1 mm particles are limited to a narrow range of solid residence times, between 0.25 s and 0.45 s. This is due to the high slip velocity of the 1.1 mm particles.

3.2.2. Solid consumption regime

Pictures of the initial wood and of a solid residue obtained after pyrolysis are shown in Fig. 13.

The particle of residue is darkened only on its edge on a thickness of about 0.1 mm after 0.45 s at 1073 K. Its centre still looks like wood. There seems to be a front of reaction moving towards the particle centre. This suggests

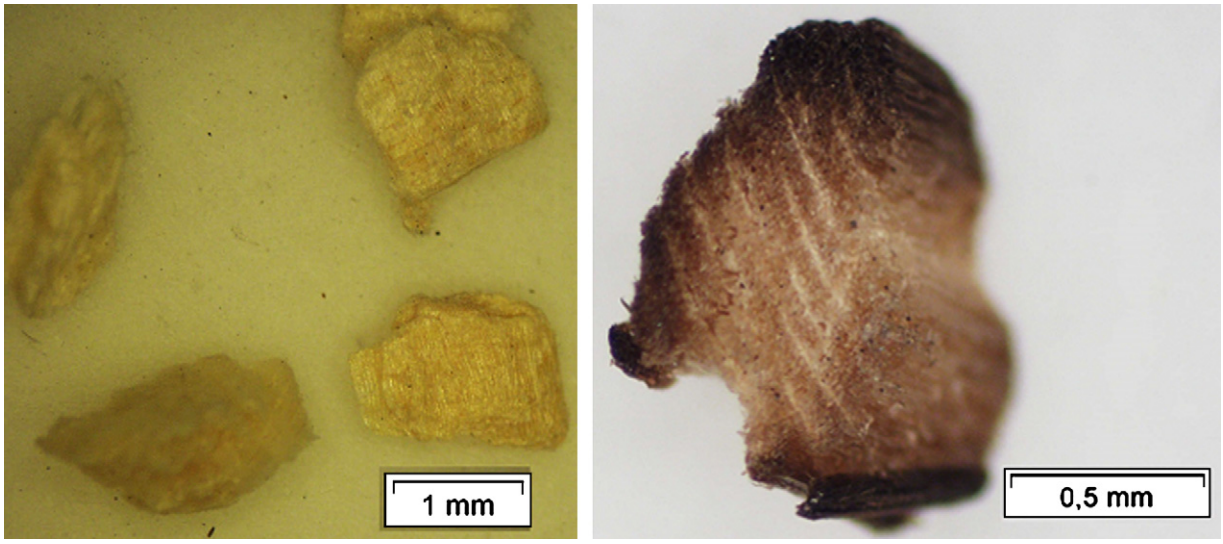

Fig. 13. Left: initial wood (1.1 mm); Right: wood particle after pyrolysis ($T = 1073$ K; solid residence time = 0.45 s).

limitations by internal heat transfers. This seems to be in agreement with the characteristic time of internal conduction calculated for particles of 1.1 mm, that is about 0.1–1.0 s [21].

3.2.3. Influence of temperature

At 1073 K, some particles are only partially darkened, whereas at 1223 K, all of them are completely darkened, as shown in Fig. 14. It can also be noticed in Fig. 15 that the edges of the particles tend to have a black gleaming aspect, as if they had molten. This observation seems to be in agreement with the mechanism of wood melting, already mentioned concerning the 0.4 mm particles.

3.2.4. Evolution of the particle size

Measurements of granulometry by laser have been made on initial wood and residue. As can be seen in Table 5, there is a significant shrinking. The increase of temperature clearly favours the shrinking of the particles.

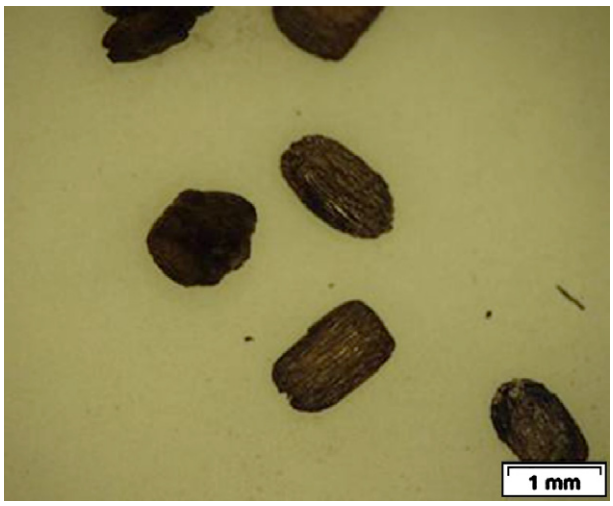

Fig. 14. Wood particles after pyrolysis ($T = 1223$ K; solid residence time = 0.45 s).

3.2.5. Results concerning gases

Gas yields are given in Table 6 for different temperatures (1073 K; 1223 K) and solid residence times.

Fig. 15. Wood particle after pyrolysis ($T = 1223$ K; solid residence time = 0.45 s).

Table 5
Shrinking of wood particles after pyrolysis (based on granulometry measurements by laser)

Temperature	K	1073	1223
Solid residence time	s	0.45	0.45
Relative shrinking[a]	%	7	15
Volume shrinking[b]	vol%	20	43

[a] $$\text{Relative shrinking} = \frac{\text{initial particle size} - \text{residue size}}{\text{initial particle size}} \times 100. \quad (3)$$

[b] The particle is considered as a homogeneous sphere.

Table 6
Gas yields for pyrolysis of 1.1 mm particles

Temperature	K	1073	1073	1073	1223	1223	1223
Solid residence time	s	0.3	0.4	0.45	0.3	0.4	0.45
Total mass of wet gas	w% of biomass	14	18	20	19	25	35
Total mass of dry gas	w% of biomass	2	4	8	9	15	25
H_2	mol/mol dry biomass	Nd[a]	Nd	0.04	0.1	0.2	0.35
CO	mol/mol dry biomass	0.1	0.2	0.3	0.4	0.6	1.0
CO_2	mol/mol dry biomass	Nd	Nd	0.01	0.02	0.05	0.08
CH_4	mol/mol dry biomass	0.01	0.02	0.05	0.06	0.10	0.17
C_2H_4	mol/mol dry biomass	0.01	0.02	0.03	0.03	0.05	0.09
C_2H_2	mol/mol dry biomass	0.004	0.008	0.015	0.03	0.04	0.07
H_2O	mol/mol dry biomass	1.1	1.2	1.1	0.8	0.9	0.8

[a] Not detected.

Under the conditions of study ($1073 < T < 1223$ K; solid residence time: 0.25–0.50 s), the maximum total gas yield is of 35 wt% of the initial biomass, which is about half of the conversion observed for 0.4 mm particles. The dry gas yield is clearly favoured by the increase of temperature and residence time. This shows that the reaction is still in progress after 0.45 s under these conditions of temperature, which is in agreement with the observations made on solid residues.

Trends are similar when each component of the dry gas is considered separately. On the contrary, the yield of steam does not seem to depend on residence time and its amount slightly decreases with temperature, from 1.1 mol/mol dry biomass to 0.9 mol/mol dry biomass. These values are comparable with the amount of water contained in biomass as moisture, which is of about 0.75 mol/mol dry biomass. This would mean that the measured steam mainly comes from drying, which is finished at 0.30 s. Drying and pyrolysis would therefore occur almost sequentially under these conditions of temperature (1073 K;1273 K) for particles of 1.1 mm. This assumption seems coherent with the observations of Visentin [1]. Indeed, this author asserts that during his experiments in EFR, under conditions slightly different from ours ($T = 673$–923 K; particle size: 0.09–0.18 mm), less than 0.10 s is necessary for drying completion.

A comparison is made in Table 7 between the dry gas yields obtained with the two particle sizes under comparable conditions.

The gas composition is relatively similar for particles of 0.4 mm and of 1.1 mm. However, there are some differences on the yield of H_2. The yield is reduced by a factor of 3 at 1073 K from the particles of 0.4 mm to those of 1.1 mm. At 1223 K, the trend is identical but not so strongly marked, with a difference of only 20%. On the contrary, CO is present in higher proportions for the biggest particles, especially at 1073 K. It could be suggested that CO would be mainly produced by the solid decomposition itself, that is primary pyrolysis, and that occurs on the biggest particles, whereas H_2 would be partly produced by the reactions between primary volatiles. These reactions do not have time to take place inside the reactor on the biggest particles.

Table 7
Dry gas composition versus particle size

Particle size	mm	0.4	1.1	0.4	1.1
Temperature	K	1073	1073	1223	1223
Solid residence time	s	0.45	0.45	0.45	0.45
H_2	mol dry gas %	21.6	8.2	26.4	20.0
CO	mol dry gas %	56.8	69.2	52.8	56.7
CO_2	mol dry gas %	4.2	2.7	4.0	4.7
CH_4	mol dry gas %	10.2	9.8	10.0	9.8
C_2H_4	mol dry gas %	5.1	7.1	3.5	4.9
C_2H_2	mol dry gas %	2.1	3.0	3.3	3.8

4. Conclusion

Flash pyrolysis experiments under N_2 and a mixture of N_2 and steam were conducted using a mixture of softwoods in an entrained flow reactor in the range of temperatures between 1073 K and 1273 K. The results are very dependent on the particle size in the range under study: 0.4 mm and 1.1 mm.

Under the conditions of study ($1073\ \text{K} < T < 1273$ K), the decomposition of the 0.4 mm particles seems to be finished after a solid residence time smaller than 0.5 s, whereas the decomposition of the 1.1 mm particles does not reach completion at 0.5 s. For the 1.1 mm particles, the decomposition is clearly limited by heat transfers; drying is apparently finished at 0.3 s. For the 0.4 mm particles, no conclusion can be drawn about the regime of decomposition since the decomposition is already finished at the smallest residence time investigated.

For the 0.4 mm particles, more than 75 wt% of the initial mass of biomass is converted into gas. Thus, there is very few solid residue remaining for gasification with steam: less than 10 wt% of the initial biomass. Moreover, this means that the products obtained during biomass steam gasification are mainly those resulting from pyrolysis and gas phase reactions.

It has also been shown that the main gas phase species produced during pyrolysis do not significantly evolve under the studied range of gas residence time that is of a few seconds. Only H_2 seems to be notably influenced, probably due to reactions with light hydrocarbons such as C_2 and

with tars that are not measured here. The other possible reactions seem to be kinetically blocked, notably the steam reforming of CH_4 and the steam cracking of C_2. The water–gas shift reaction is kinetically controlled at 1073 K and is close to equilibrium at the highest temperature and gas residence time investigated (1273 K, 3.5 s); it is clearly favoured by the presence of an excess of steam.

References

[1] Visentin V, Piva F, Canu P. Experimental study of cellulose fast pyrolysis in a flow reactor. Ind Eng Chem Res 2002;41:4965–75.

[2] Cetin E, Moghtaderi B, Gupta R, Wall TF. Influence of pyrolysis conditions on the structure and gasification reactivity of biomass chars. Fuel 2004;83(16):2139–50.

[3] Brink DL, Massoudi MS. A flow reactor technique for the study of wood pyrolysis. I. Experimental. J Fire Flammability 1978;9:176–88.

[4] Van de Steene L. Thermochimie de la combustion à basses températures de solides pulvérisés: application à un charbon. PhD thesis 1999. Institut National Polytechnique de Toulouse: Toulouse, France.

[5] Zanzi R. Pyrolysis of biomass: rapid pyrolysis at high temperature; slow pyrolysis for active carbon preparation. PhD thesis 2001. Royal Institute of Technology: Stockholm, Sweden.

[6] Van de Steene L, Salvador S, Napoli A. Rice husk straw and bark behaviour during pyrolysis combustion and gasification: fundamental study. In: 12th European Conference on Biomass for Energy, Industry and Climate Protection. Amsterdam, The Netherlands: 2002.

[7] Pillet S. Réalisation d'un système expérimental pour caractériser la combustion et les émissions d'oxydes d'azote des combustibles solides: application aux charbons et à la biomasse PhD thesis 2005. Université d'Orléans: Orléans, France.

[8] Bohn M, Benham C. An experimental investigation into fast pyrolysis of biomass using an entrained-flow reactor. 1981. Solar Energy Research Institute, US Department of Energy.

[9] Bitowft B, Andersson LA, Bjerle I. Fast pyrolysis of sawdust in an entrained flow reactor. Fuel 1989;68:561–6.

[10] Hayashi JI, Iwatsuki M, Morishita K, Tsutsumi A, Li CZ, Chiba T. Roles of inherent metallic species in secondary reactions of tar and char during rapid pyrolysis of brown coals in a drop-tube reactor. Fuel 2002;81:1977–87.

[11] Li S, Xu S, Liu S, Yang C, Lu Q. Fast pyrolysis of biomass in a free-fall reactor for hydrogen-rich gas. Fuel Process Technol 2004;85:1201–11.

[12] Hallgren A, Andersson LA, Bjerle I. High temperature gasification of biomass in an atmospheric entrained flow reactor. In: Bridgwater AV, editor. Advances in thermochemical biomass conversion. Cambridge: Blackie Academic and Professional; 1993.

[13] Shuangning X, Zhihe L, Baoming L, Weiming Y, Xueyuan B. Devolatilization characteristics of biomass at flash heating rate. Fuel 2006;85(5–6):664–70.

[14] Commandré JM. Formation des oxydes d'azote lors de la combustion de cokes de pétrole dans des conditions de précalcinateur de cimenterie. PhD thesis 2002. Institut National Polytechnique de Toulouse: Toulouse, France.

[15] Dupont C. Vapogazéification de la biomasse : contribution à l'étude de la phénoménologie entre 800 et 1000 °C. PhD thesis 2006. Université Claude Bernard: Lyon, France.

[16] Biagini E, Tognotti L. Characterization of biomass chars: reactivity and morphology of chars obtained in different conditions clean air. Int J Energ Clean Environ 2005(4):439–57.

[17] Lin W, Dam-Johansen K, Frandsen F. Agglomeration in bio-fuel fired fluidized bed combustors. Chem Eng J 2003;96(1–3):171–85.

[18] Natarajan E, Nordin A, Rao AN. Overview of combustion and gasification of rice husk in fluidized bed reactors. Biomass Bioenergy 1998;14(5–6):533–46.

[19] Lédé J, Li HZ, Villermaux J. Fusion-like behaviour of wood pyrolysis. J Anal Appl Pyrol 1987;10:291–308.

[20] Boutin O, Ferrer M, Lédé J. Radiant flash pyrolysis of cellulose – evidence for the formation of short life time intermediate liquid species. J Analy Appl Pyrol 1998;47:13–31.

[21] Dupont C, Boissonnet G, Seiler JM, Gauthier P, Schweich D. Study about the kinetic processes of biomass steam gasification. Fuel 2006;86(1–2):32–40.

[22] Hofbauer H, Rauch R, Foscolo P, Matera D. Hydrogen rich gas from biomass steam gasification. In: 1st World conference and exhibition on biomass for energy and industry, Sevilla, Spain; 2000.

[23] Ravel S. Gazéification de la biomasse pour la synthèse et la production de carburants renouvelables (projet GASPAR). Volet 3: Vapogazéification en lit fluidisé. Rapport d'essai T0+14: Caractérisation du LFHT suite au premier essai avec injection de biomasse. 2006, CEA: Grenoble, France.

[24] Stoltze S, Henriksen U, Lyngbech T, Christensen O. Gasification of straw in a large-sample TGA. In: Proceedings of the Nordic seminar on solid fuel reactivity, Gothenburg, Sweden; 1993.